CHAPTER IV

PRODUCTIONS OF PETROCHEMICALS AND DISTILLATE RANGE OF HYDROCARBONS FROM BIO-ETHANOL DEHYDRATION USING THREE ACID SUPPORTS DOPED WITH OXIDES OF GROUP 5A

4.1 Abstracts

HZSM-5 has the potential in the dehydration of ethanol to gasoline (ETG) because of its proper acid property and shape selectivity. It had been used as support of phosphorus oxide, antimony oxide, and bismuth oxide for ethanol dehydration, which mainly gave oils in gasoline range. It can be noticed that the moderate pore size of HZSM-5 limits the production of heavier oils in the kerosene and gas oil ranges. Therefore, in this work, the large pore size zeolites, HY and HBeta, were expected to produce larger hydrocarbon molecules. Then, bio-ethanol dehydration using HY, HBeta, and HZSM-5 doped with phosphorus oxide, antimony oxide, and bismuth oxide was investigated, aiming to improve the production of distillate-range products. The reaction was carried out in an isothermal fixed-bed reactor. The temperature was controlled at 500 $^{\circ}$C, and the LHSV was fixed at 0.5 h^{-1} Phosphorus oxide, antimony oxide, and bismuth oxide (5 wt.%) were loaded to all zeolites using incipient wetness impregnations. The characterization techniques; XRD, XPS, XRF, SAA, TPD-IPA were used to characterize the catalysts. The products were analyzed by using GC, GC×GC-MS/TOF and SIMDIST GC. As a result, HZSM-5 gave more oil yield than HY, and HBeta.

4.2 Introduction

Depleting reserve of petroleum nowadays makes the world face with high price of the conventional fuels; that are, gasoline, kerosene, and gas oil. Bio-fuel, especially ethanol, is one of high potential, renewable petroleum substitutes to solve the problems. Corn crop, sugarcane, and other agriculture wastes and by-products can be utilized to produce bio-ethanol. Purified bio-ethanol is used to blend with

gasoline to become in E10, E20, and E85 gasohol, used directly in some types of vehicles.

Moreover, ethanol can be the feedstock of some valuable petrochemical products via the catalytic dehydration process. Several research articles focused on ethylene (Bi *et al.*, 2010; Sheng *et al.*, 2013) and propylene (Furumoto *et al.*, 2011; Meng *et al.*, 2012) productions using modified ZSM-5 catalysts. Moreover, the oil product that can be separated to petroleum fractions may also contains highly valuable products. Costa *et al.* (1985) studied the catalytic dehydration of ethanol to gasoline by using HZSM-5 as a catalyst. The results showed that the zeolite with moderate SiO_2/Al_2O_3 (42.5) ratio produced the highest liquid yield, and the recycle gas phase system can increase the conversion of gas phase, and increase liquid hydrocarbon yields up to 67%. Moreover, the liquid product was increased up to 70% with introducing the high pressure (20atm) to the system. The high pressure can help to yield the paraffin product; however, the aromatic product was decreased. Johansson *et al.* (2009) investigated that the product distributions in cases of methanol to gasoline (MTG) and ethanol to gasoline (ETG) using HZSM-5 ($SiO_2/Al_2O_3 = 23$) as a catalyst were similar in terms of the product species in both gas and liquid. However, they noticed about some differences that dimethylether was formed in MTG, but ethylene was formed in ETG. In addition, they proposed that bio-ethanol can blend with methanol to be a feedstock for MTG plants.

Park and Seo (2009) studied the methanol to olefin (MTO) reaction by using different types of zeolites, which are CHA, LTA, MFI, BEA, MOR, and FAU. They investigated that the MTO over CHA, LTA, and MOR were selective to olefins. Moreover, CHA showed the best performance by maintaining the selectivity to light olefins without deactivation of catalysts. However, MFI and BEA were selective to aromatic compounds. In addition, HY that initially produced light olefins produced aromatics mainly at after the 200 minutes time on streams. Ethanol is much more attractive than methanol since it can be converted to larger hydrocarbons such as diesel and jet fuel (Güell *et al.*, 2012). It was proposed that the way to convert ethanol to jet via dehydration process was to convert ethanol to ethylene first, and then convert ethylene to larger olefin via oligomerization at moderate temperatures and pressures (150-250°C, 3-4 MPa). Polynaphtha[TM] and AlphaSelect[TM] are the

examples of commercial processes for this application. They convert light olefins to gasoline and kerosene under mild operating conditions by using a series of fixed bed reactors. A Zr-based catalyst and an amorphous silica-alumina (ASA) catalyst were reported to be used in Polynaphta^{TM} via liquid phase reaction under moderate temperatures and pressures. In addition, the Catalytic Polymerisation (CatPoly) technology of UOP based on olefin oligomerization by using a solid phosphoric acid (SPA) as a catalyst has also been commercially available (de Klerk, 2008).

Aiming to produce distillate range product, Pasomsub (2013) found that kerosene and larger hydrocarbons (kerosene$^+$) were produced by using HZSM-5 ($SiO_2/Al_2O_3 = 40$), a moderate pore size zeolite, doped with one of group 5A oxides (P-, Sb-, and Bi- oxide) at 1-4% loading (elemental basis). For HZSM-5 supported phosphorus oxide, he found that kerosene and gas oil decreased with the increasing percentage loading of phosphorus oxide. However, kerosene and gas oil productions were improved with the introduction of antimony oxide and bismuth oxide to the HZSM-5. The kerosene contents were 19.5% and 22.0% in oil with using HZSM-5 supported antimony oxide and bismuth oxide, respectively. In addition, SAPO-34 (the 1D small pore size zeolite) supported 5% antimony oxide catalysts yielded kerosene-range products up to 2.87%, and improved the liquid yield to 8.51% as compared with pure SAPO-34 that prohibited the oil production (Wongwanichsin, 2013).

Furthermore, some large pore size zeolites, which are HY and HBeta, were reported to enhance kerosene$^+$ products (Madeira *et al.*, 2009) from ethanol transformation. They found that C_5-C_{11} was yielded mostly by HZSM-5; however, C_{12}^+ was found mostly by using HY and HBeta at the early of the reaction. They also claimed that C_{12}^+ hydrocarbons were almost the aromatic compounds. Thus, in this work, the catalytic dehydration of bio-ethanol using HY and HBeta zeolites doped with group 5A oxides were investigated in the attempt to increase the kerosene$^+$ products, and the results were also compared with using HZSM-5 as a support in order to investigate the effect of pore size and structure of zeolites. All zeolites used had a very similar value of SiO_2/Al_2O_3 ratio (27-30) in order to avoid the effect of acid properties of zeolites.

4.3 Experimental

4.3.1 Catalyst Preparation

HZSM-5 zeolite (MFI, NH_4-form, SiO_2/Al_2O_3 = 30 mol/mol, BET surface area = 405 m^2/g, Zeolyst International, USA), HY zeolite (FAU, H-form, SiO_2/Al_2O_3 = 30 mol/mol, BET surface area = 780 m^2/g, Zeolyst International, USA), HBeta (BEA, H-form, SiO_2/Al_2O_3 = 27 mol/mol, BET surface area = 600 m^2/g, TOSOH, Singapore) were used in this work. HZSM-5 was calcined at 500°C, 5 °C/min for 3 hour was and HBeta were calcined at 500°C, 10 °C/min for 3-5 hours, and HY was calcined at 500 °C, 5 °C/min for 3 hours to get the H-form zeolite and remove the impurity. The diammonium hydrogen phosphate (($NH_4)_2HPO_4$, CARLO ERBA), antimony trichloride ($SbCl_3$, CARLO ERBA), and bismuth trichloride ($BiCl_3$, ALDRICH) were used as the sources of P, Sb, and Bi, respectively. A solution of these compounds was individually loaded on the supports using the incipient wetness impregnation technique until the final loading amount of 5.0 wt % (elemental basis) was achieved. After impregnation, wet catalysts were dried in an oven at 100 °C for 1 hours followed by calcination at 500°C, 10 °C/min for 3 hours. Then, the calcined sample was hydraulically pressed to pellets. Subsequently, the pellets were crushed and sieved to 20 - 40 mesh particles before use in the reactor. The abbreviations of catalysts used in the experiment are shown in Table 4.1.

4.3.2 Catalyst Characterization

The surface area (BET), pore volume (HK), and pore size (HK) were determined based on N_2 physisorption using the Thermo Finnigan/Sorptomatic 1990. Crystallographic spectra of the zeolites were determined using Rigaku SmartLab® in BB/Dtex mode with $CuK\alpha$ radiation. The machine collected the data from $5^\circ - 90^\circ$ at 10°/min with the increment of 0.01°. XPS was used to determine the oxidation states of metal oxides dispersed in zeolites. The scan pass energy was 160 kv for wide scan and 40 kv for narrow scan. The electron source was Al $K\alpha$ that gave 10 mA of emission and 15 kV of anode HT. The neutralizer was set at 1.8 A of filament current, 2.6 V of charge balance, and 1.3 V of filament bias. The amount of elemental loading on zeolites was determined by using XRF (AXIOS PW4400) with the radiation at 50 kv 60 mA.

Table 4.1 Nomenclature of catalysts used in the experiments

# of run	Catalyst	Abbreviation
1	HZSM-5(SiO_2/Al_2O_3 = 30)	HZ5
2	HBeta(SiO_2/Al_2O_3 = 27)	HBeta
3	HY(SiO_2/Al_2O_3 = 30)	HY
4	5% Phosphorus oxide/HZSM-5(SiO_2/Al_2O_3 = 30)	P/HZ5
5	5% Antimony oxide/HZSM-5(SiO_2/Al_2O_3 = 30)	Sb/HZ5
6	5% Bismuth oxide/HZSM-5(SiO_2/Al_2O_3 = 30)	Bi/HZ5
7	5% Phosphorus oxide /HBeta(SiO_2/Al_2O_3 = 27)	P/HBeta
8	5% Antimony oxide / HBeta(SiO_2/Al_2O_3 = 27)	Sb/HBeta
9	5% Bismuth oxide / HBeta(SiO_2/Al_2O_3 = 27)	Bi/HBeta
10	5% Phosphorus oxide /HY(SiO_2/Al_2O_3 = 30)	P/HY
11	5% Antimony oxide /HY(SiO_2/Al_2O_3 = 30)	Sb/HY
12	5% Bismuth oxide /HY(SiO_2/Al_2O_3 = 30)	Bi/HY

4.3.3 Bio-ethanol Dehydration

The fuel grade bio-ethanol (99.5% purity) was obtained from Sapthip co., ltd., Thailand. The catalytic dehydration of bio-ethanol was conducted in a U-tube fixed bed reactor (10 mm, inside diameter and 45.8 cm, length) under atmospheric pressure at 500°C for 8 hours. Helium was used as a carrier gas fed at 13.725 ml/min. Bio-ethanol was fed at 2 ml/hour. 3 grams of catalyst was used in the reaction. The gas product was analyzed by using a GC-TCD (Agilent 6890N) to determine the gas compositions, and a GC-FID (Agilent 6890N) was used to determine the ethanol concentration in gas stream. The liquid product was condensed in the collector immerged in an ice-salt bath, and then the oil phase was extracted from the liquid product using CS_2. The oil was next analyzed by using GC×GC- MS / TOF (Rxi-5SilMS, and RXi-17) to determine its composition. Moreover, the true boiling point curve of oil was determined by using SIMDIST GC. The range of boiling points indicates the type of petroleum products; <120 °C for gasoline, 149-232 °C for kerosene, 232-343 °C for gas oil, 343-371 °C for light vacuum gas oil, and >371 °C for high vacuum gas oil (Pasomsup, 2013).

## 4.4 Results and Discussion

4.4.1 Catalyst Characterization

Table 4.2 Physical properties of pure zeolites and group 5A modified-zeolites

Catalyst⁻	Surface area (m^2/g) [a]	Pore volume (cm^3/g) [b]	Pore diameter (Å)
HY	658.7	0.3333	7.975
P/HY	346.7	0.1695	7.835
Sb/HY	581.1	0.2909	8.467
Bi/HY	570.4	0.2853	8.487
HBeta	498.1	0.2501	8.154
P/HBeta	347.1	0.1675	7.087
Sb/HBeta	482.6	0.2341	9.372
Bi/HBeta	474.6	0.2293	8.493
HZ5	359.1	0.1590	8.968
P/HZ5	188.2	0.0915	6.897
Sb/HZ5	280.4	0.1444	9.024
Bi/HZ5	195.2	0.0934	6.394

[a] determined using BET method
[b] determined using HK method

The BET surface area and pore volume decrease when zeolites are doped with group 5A oxides as shown in Table 4.2. The higher molecular weight of group 5A in oxide loaded, the larger the surface area and pore volume decrease. In addition, the small molecular size of phosphorus oxide leads to the high deposition in the pore of zeolite, so, the surface area and pore volume are highly decreased. Moreover, the pore diameter is increased when antimony oxide, or bismuth oxide is used as a promoter; however, phosphorus oxide doping decreases the pore diameter of all types of zeolite.
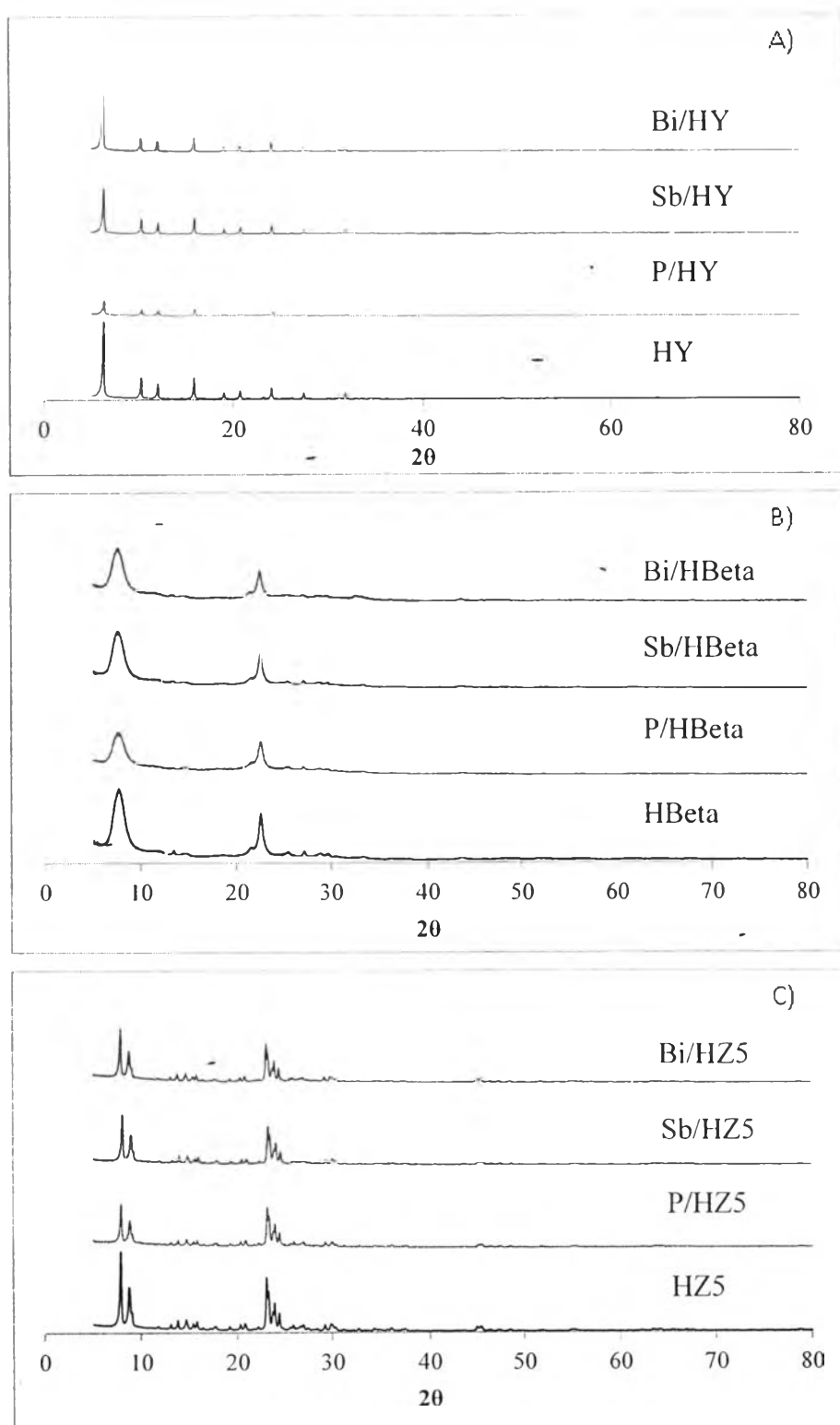
Figure 4.1 Crystallographic spectra of phosphorus oxide-, antimony oxide-, and bismuth oxide-modified HY(A), HBeta(B), and HZSM-5(C).
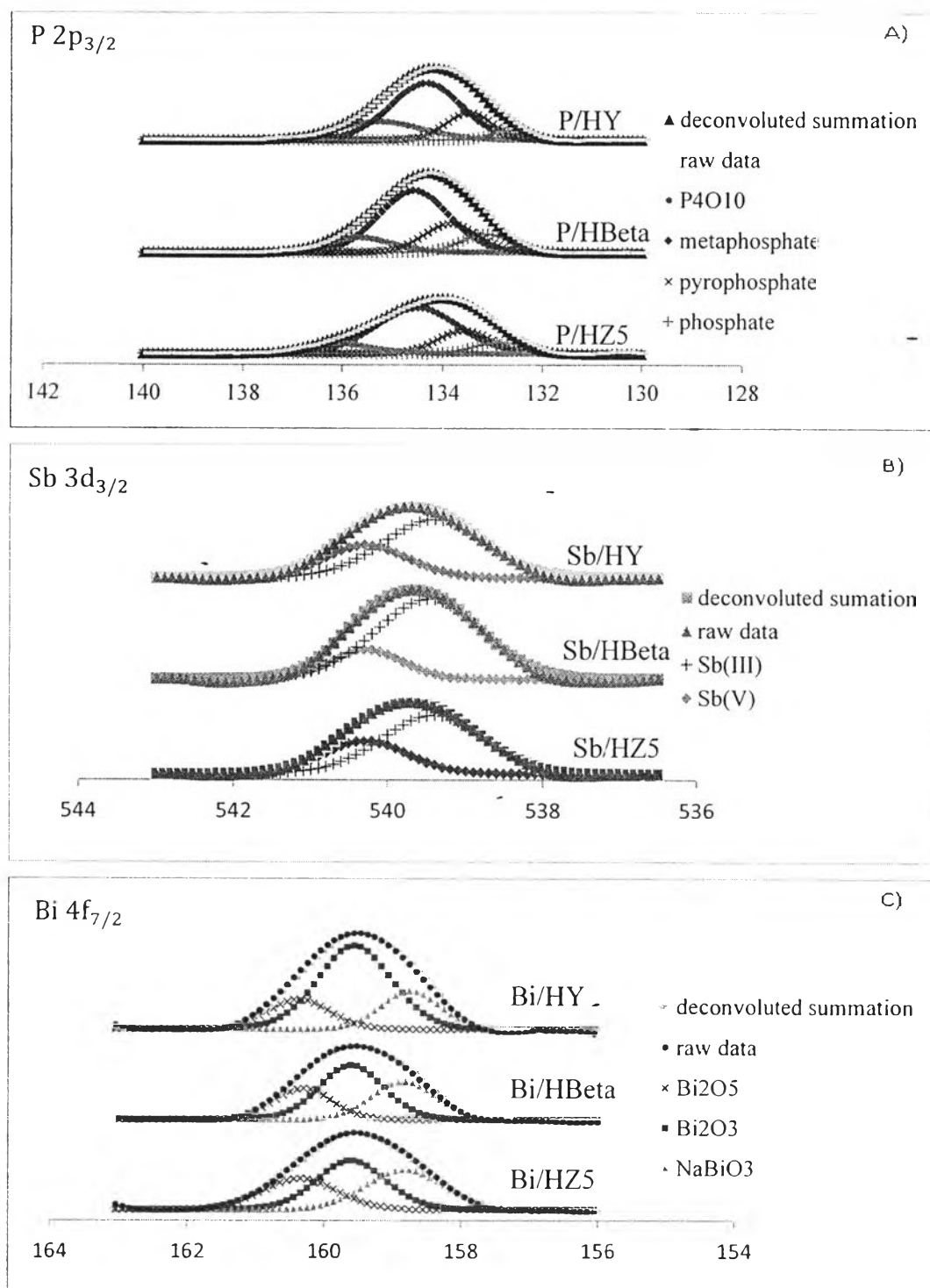
Figure 4.2 XPS spectra of (A) phosphorus oxide-, (B) antimony oxide-, and (C) bismuth oxide-doped catalysts.

The XRD spectra are shown in Figure 4.1. The characteristic peaks of HY are located at $6.34°$, $10.33°$, and $15.94°$, and those of HBeta are $7.74°$, $12.24°$, and $22.09°$ whereas those of HZSM-5 are at $7.94°$, $8.89°$, $14.77°$, and $23.96°$. The XRD patterns of pure zeolites and corresponding modified zeolites show the same 2θ of identity peaks. So, the modification of the zeolites did not destroy the structure of the zeolites.

The oxidation state of oxides on the modified zeolites is determined by using XPS, and the results are shown in Figure 4.2. XPS spectra of phosphorus oxide-modified catalysts illustrate the P $2p_{3/2}$ binding energies at 135.8, 134.7, 133.3, 132.4 eV that can be interpreted to P_4O_{10}, metaphosphate, pyrophosphate, and phosphate, respectively (Moulder et $al.$, 1992). Zhang et $al.$ (2013) reported that the Sb $3d_{3/2}$ positions at 540.4 eV and 539.6 eV can be interpreted to Sb_2O_5 and Sb_2O_3, respectively. The Sb $3d_{5/2}$ spectrum is found to overlap with O 1s that occurs at 531.0 eV (Moulder et $al.$, 1992). However, the XPS peak of Sb $3d_{3/2}$ is considered instead of Sb $3d_{5/2}$ in the case that oxygen is the mutual element in the sample. In this case, the Sb $3d_{3/2}$ spectra of antimony oxide-supported zeolites appear at 539.5 and 540.3 eV, which can be interpreted to Sb_2O_3 and Sb_2O_5, respectively. Bismuth oxide-modified catalysts mainly contain Bi_2O_3 whose peak is located at 159.2 while other spectra appear at 160.4, 158.8 eV that refer to Bi_2O_5 and BiO_3^+, respectively.

4.4.2 Effect of zeolite type

Bio-ethanol was dehydrated over HZSM-5, HBeta, and HY with a sufficiently-close SiO_2/Al_2O_3 ratio ($SiO_2/Al_2O_3=30$ for HZSM-5, and HY, $SiO_2/Al_2O_3=27$ for HBeta) to examine the effect of pore size and structures of zeolites.

The conversion of ethanol is 96.7-99.6%. The large pore size of the zeolites tends to give higher gas yield and lower liquid yield as can be noticed in Figure 4.3. The oil yield obtained by using zeolite in ethanol dehydration is ranked as follows: HZ5>HY>HBeta. It can be seen that oil yield obtained by using HZSM-5 (7.05%) is higher than that obtained from the other supports.
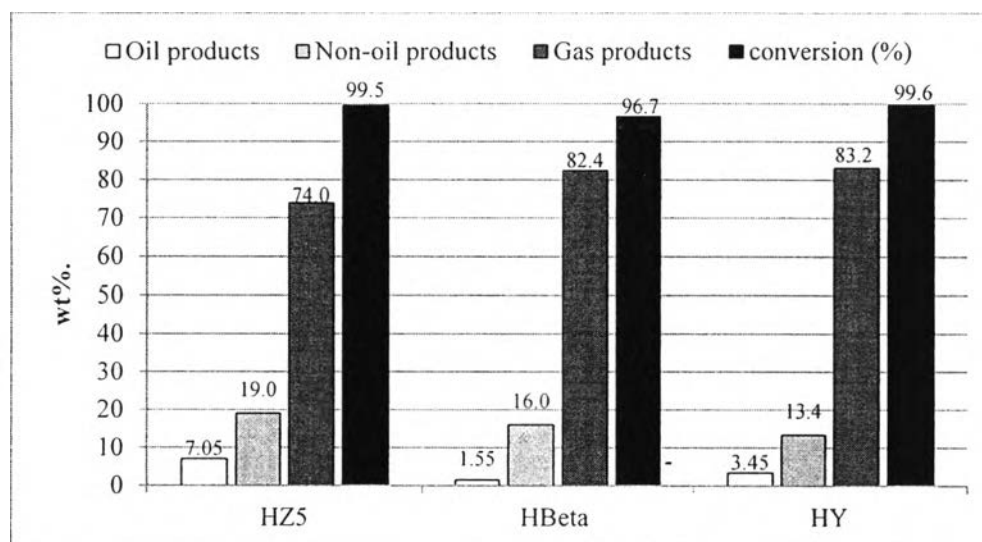
Figure 4.3 Product distribution and ethanol conversion from using HZ5, HBeta, and HY catalysts.
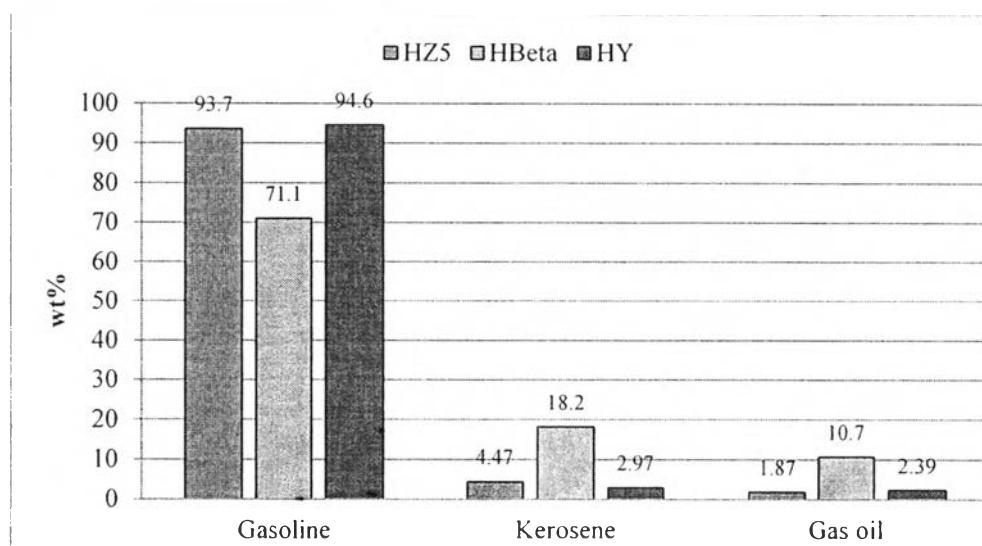
Figure 4.4 Petroleum fractions in oils from using HZ5, HBeta, and HY catalysts.

Large pore size zeolites have low contact angle of adsorbed molecule, resulting in low catalytic activity. So, the oil yield produced by using moderate pore size zeolite is higher than large pore size zeolite. Moreover, the oil obtained by using HZSM-5 contains 93.7% gasoline as shown in Figure 4.4. The highest selectivity of distillate-range is observed with using HBeta as the catalyst. HBeta, which is large

pore size with straight channel structure, can yield the large hydrocarbon molecule due to its low complexity of pore channel that leads to low cracking activity. HY is also a large pore size zeolite, but its zig-zag channel structure promotes the cracking activity, resulting in low the selectivity of oil in distillate-range.
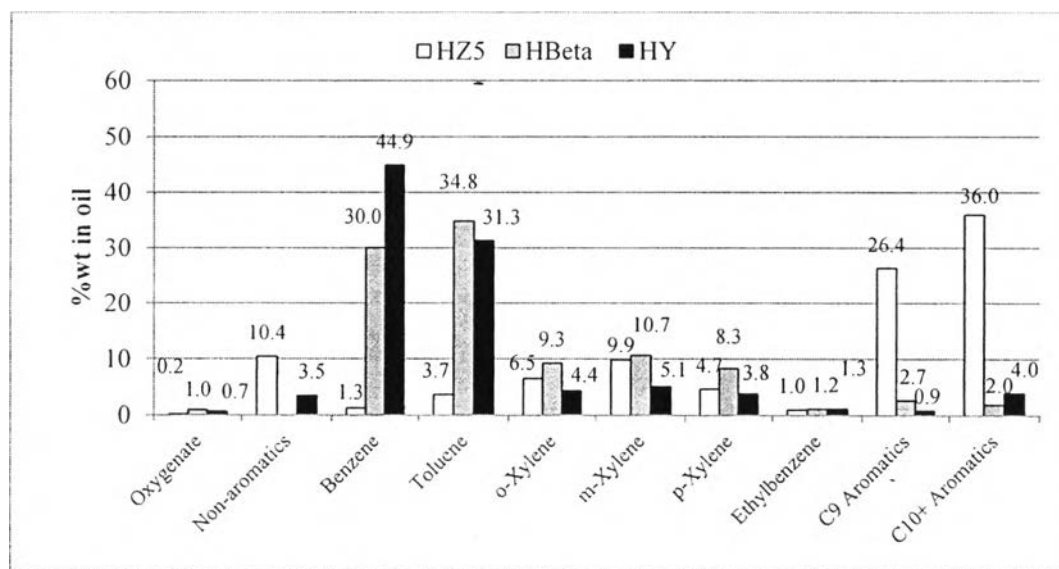
Figure 4.5 Composition of extracted oils from using HZ5, HBeta, and HY catalysts.

The oil compositions obtained by using unmodified zeolites in ethanol dehydration are shown in Figure 4.5. Benzene selectivity is increased along the increasing pore size. The pore size of HZSM-5 is normally proper to p-xylene production (Van Vu *et al.*, 2006); however, in this case, HZSM-5 produced a lot of C9 aromatics and C10+ aromatics along with the low selectivity of p-xylene. On the other hand, HZSM-5 still produces a considerable ratio of xylenes in BTEX (0.68) as seen in Figure 4.7. Xylenes, C9, and C10$^+$ can be produced by the Diels-Alders reaction (Cole *et al.*, 1984), and dehydrocyclization (Resasco, 2000). Moreover, these aromatic compounds can be converted to other forms via dealkylation, transalkylation, and disproportionation (Ali *et al.*, 2013). HBeta zeolite also produces high selectivity to p-xylene (p-xylene/xylene = 0.3) with the low amount of C9 and C10+ aromatics as shown in Figure 4.7 A. 40% BTEX in oil and 95% in total aromatics from using HBeta zeolite are the highest among those given by the other

supports. HY zeolite can produce a lot of benzene and toluene. This can be ascribed to its large pore size that leads to low contact angle of adsorbed molecule. So, the consequent reactions, which are oligomerization, transalkylation, and disproportionation, can slightly occur. For HZSM-5, its proper contact angle of adsorbed molecule can drive small olefins to convert to BTEX products, and some of small olefins receives hydrogen to form paraffins. The reaction pathways are illustrated in Figure. 4.6.
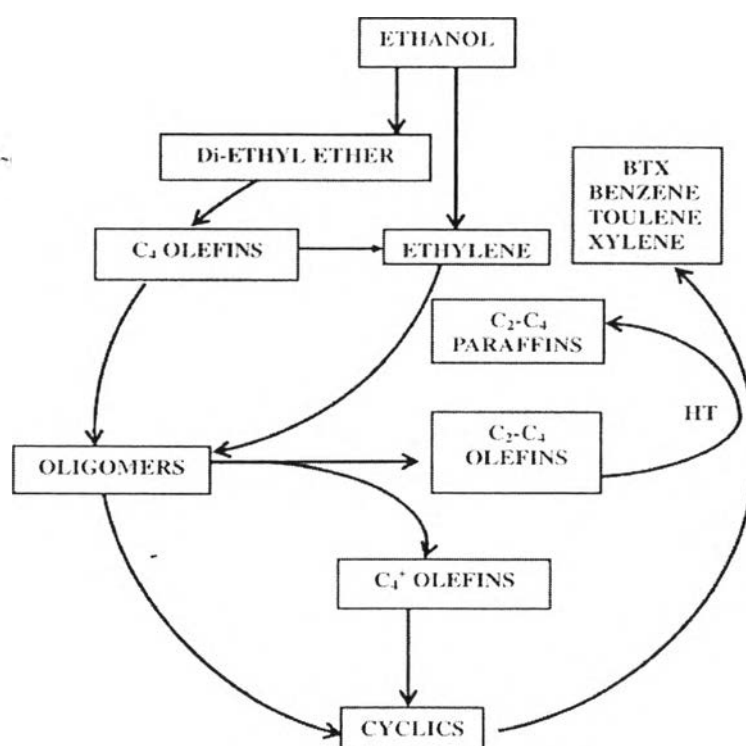
Figure 4.6 Ethanol dehydration pathways to hydrocarbons (Viswanadham *et al.*, 2012).

HZSM-5 gave a high selectivity of propane; nevertheless, propylene is observed in a low amount as shown in Figure 4.7 (B). This can be explained by hydrogen transfer to propylene to form propane, and some of propylene is protonated to form larger hydrocarbons In case of large pore size zeolite. ethylene is the main reactant even though the secondary and primary carbenium ions generated by protonation of propylene are more stable than primary carbenium ions generated by

protonation of ethylene because the high contents of ethylene lead to a high possibility to react. Propylene and methane normally are not produced from dehydration reaction directly; however, cracking of benzene and toluene can produce propylene and methane. Moreover, β-scission can produce propylene, as well. However, HY and HBeta, the large pore size zeolites, give a low aromatic yield and a high ethylene yield, which means ethylene is converted to large hydrocarbons in a lesser amount than in case of HZSM-5.
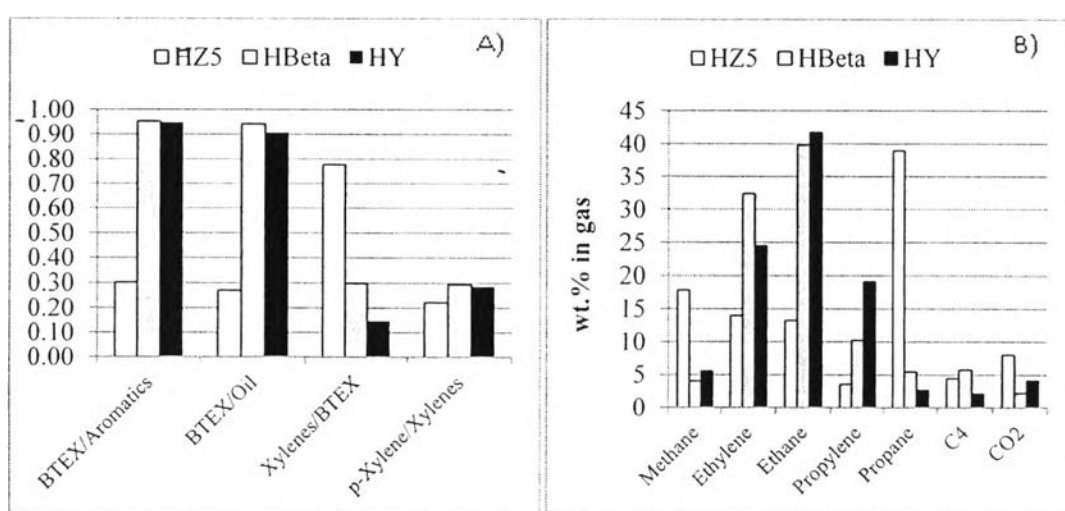
Figure 4.7 (A) BTEX ratios, and (B) gas product distribution (wt%) of pure zeolite.

4.4.3 Effect of Phosphorus Oxide Promoter

In P/HBeta, the oil yield is increased from 1.55% to 4.40% when phosphorus oxide is introduced to HBeta as shown in Figure 4.8. The oil yield can be ranked as follows: P/HBeta>P/HY>P/HZ5. This can be explained that phosphorus oxide deposits to the large pore size of HBeta and HY, which is supported by the decrease in pore diameter when phosphorus is introduced oxide as a promoter, so, the remaining pore size is much proper to produce aromatic compounds. Moreover, phosphorus oxide can increase the acid properties of a large pore size zeolite, resulting in oil yield improvement. However, phosphorus oxide accompanies to strong acid sites, and decreases the acid density of HZ5 as shown in Figure 4.9, causing P/HZ5 to give lower oil yields than pure HZ5.
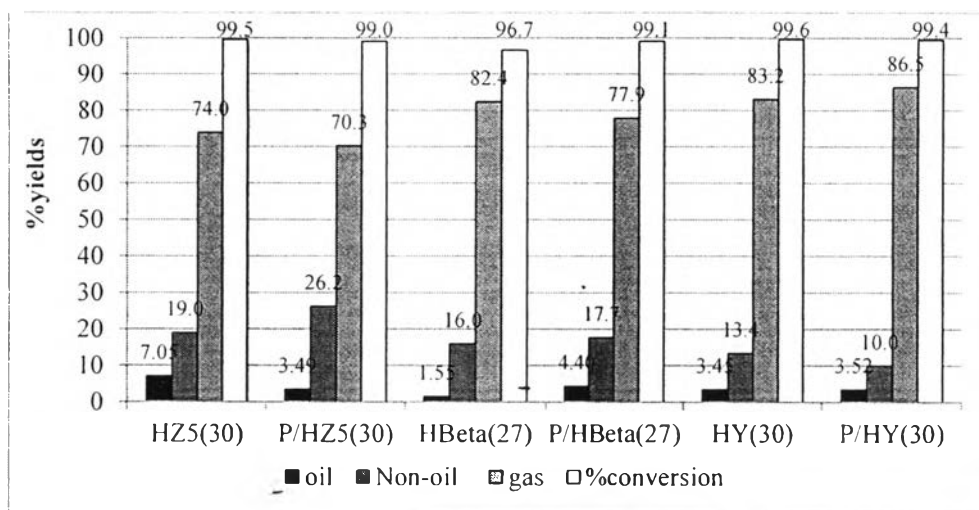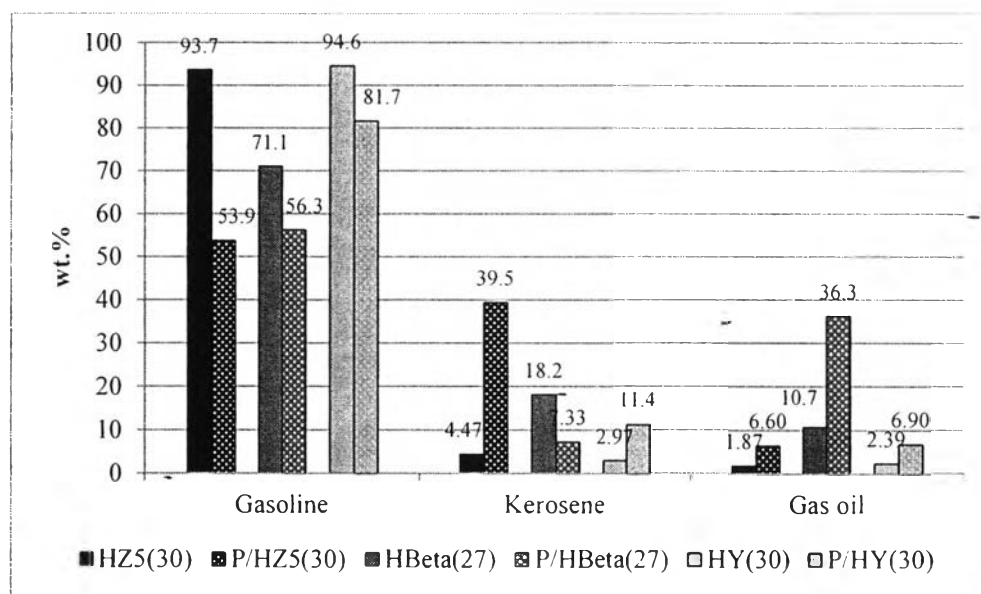
Figure 4.8 Product distribution (wt%) using P/HZ5, P/HBeta, and P/HY catalyst.
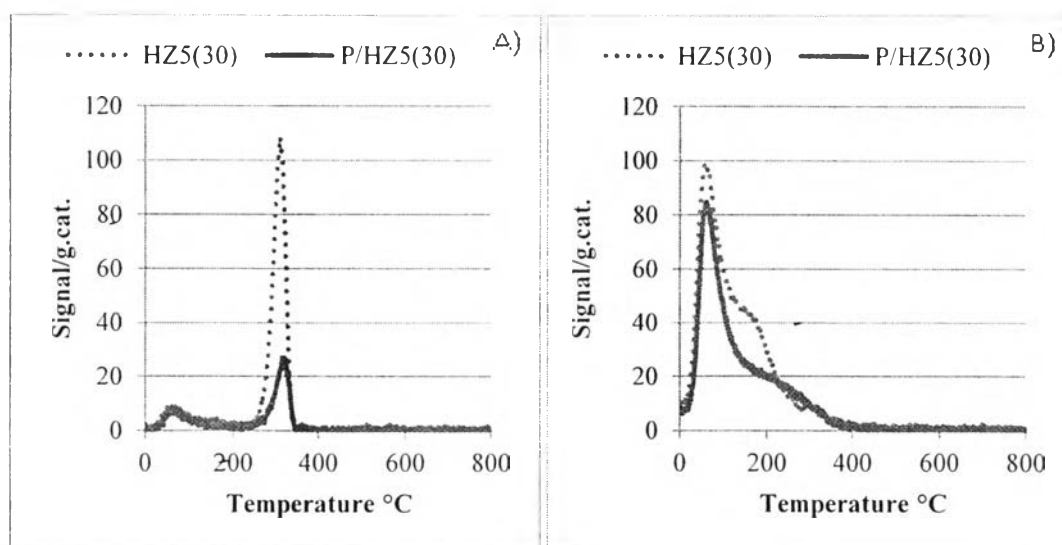
Figure 4.9 Spectra of desorbed propylene (A) and desorbed IPA (B) from using HZ5(30) and Sb/HZ5(30) in TPD-IPA tests.

P/HZ5 gives the greatest kerosene content in the oil (38.5%) with a high selectivity of C10+ aromatics. On the other hand, it gives low oil yield and BTEX products, as shown in Figures 4.8, and 4.10. P/HZ5 mainly yields kerosene; in addition. P/HBeta yields gas oil the most. In case of P/HZ5, C10+ aromatics can be assumed to generate outside the micropore, because the inside of micro pores has

larger contents of phosphorus oxide explained by capillary force in the impregnation step.

**Figure 4.10** Petroleum fractions (wt% in oils) from using P/HZ5, P/HBeta, and P/HY catalysts.

The distributions of products in oils are shown in Figure 4.11. All cases of P-oxide modified zeolites show the increases in oxygenate and C10+ aromatic products. C6 and C7 aromatics are increased while C8 and C9 aromatics are decreased by using P/HZ5. However, C7 and C8 aromatics are decreased while C9 aromatics are increased by using large pore size zeolites. C9 aromatics contents produced by using P/HZ5 seem to be limited by the modified pore size; on the other hand, this is slightly affected by the large pore size of zeolite.

It was evident that phosphorus oxide doped on HZSM-5 can cause the decrease of strong acid sites and the increase in weak acid sites (Xue *et al.*, 2007). Moreover, propylene desorption spectra also show the decrease of acid sites. So, P/HZ5 can produce the great amount of ethylene as shown in Table 4.12B. The weak acid site and oxide can participate in ethanol dehydration reaction (Inaba *et al.*, 2006).
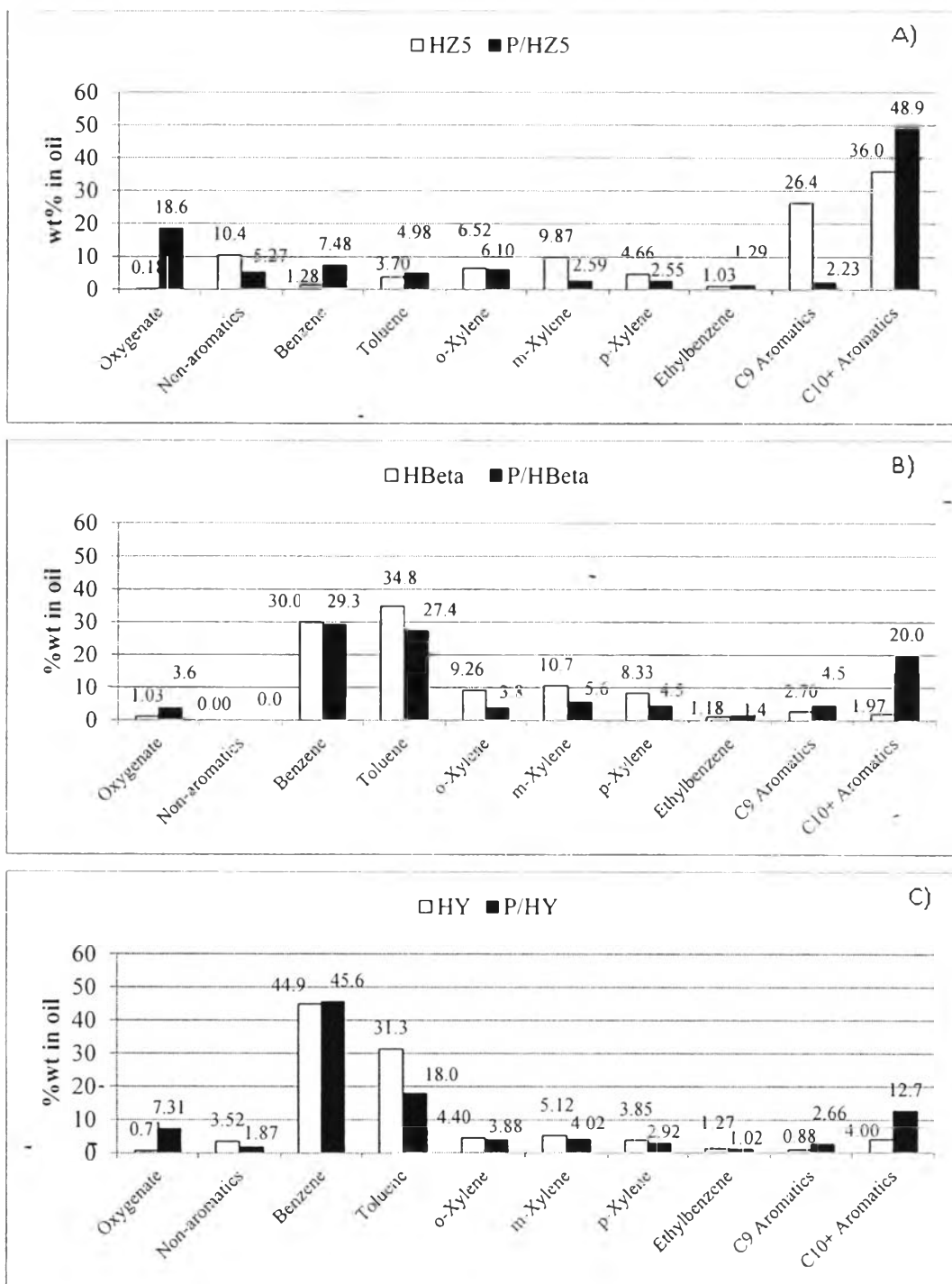
Figure 4.11 Compositions of extracted oils from using (A) P/HZ5, (B) P/HBeta, and (C) P/HY catalysts.
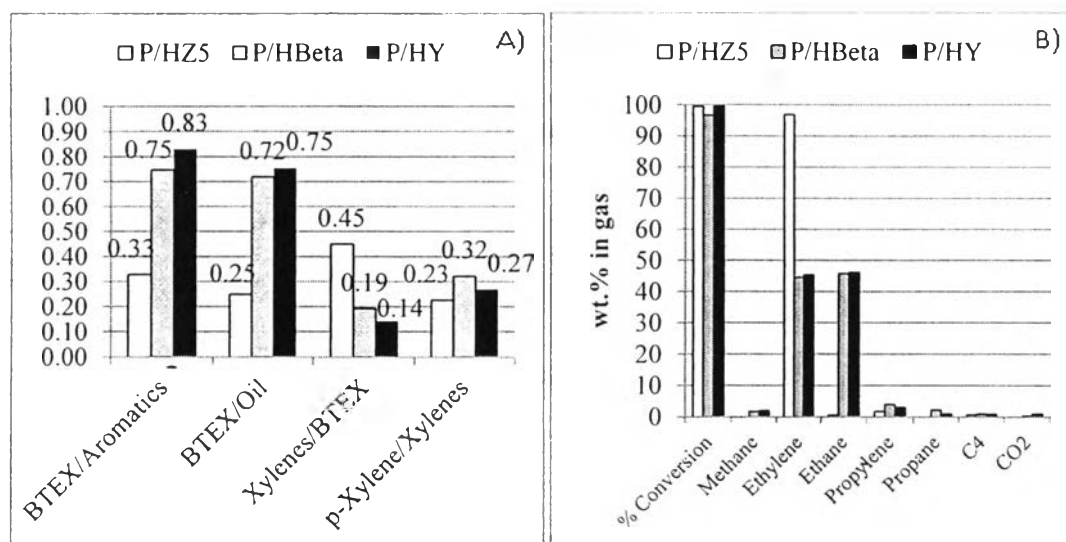
Figure 4.12 (A) BTEX ratios, and (B) gas product distribution (wt%) of phosphorus oxide-modified zeolites.

Moreover, the oxygenate product is made dominantly by P/HZSM-5 (19.39 wt.% in oil). It is composed of ketone, phenol, and cresol. The compositions of extracted oils from using P/HZ5, P/HBeta, and P/HY catalysts are shown in Figure 4.13. The main oxygenate product is 3-methyl-phenol. It holds 50% of all oxygenate compounds in oil. The total of all phenol and its derivatives is 71%. In addition, the ketone products are composed of 2-pentanone, 3-pentanone, and 2-hexanone as shown in Figure 4.13.
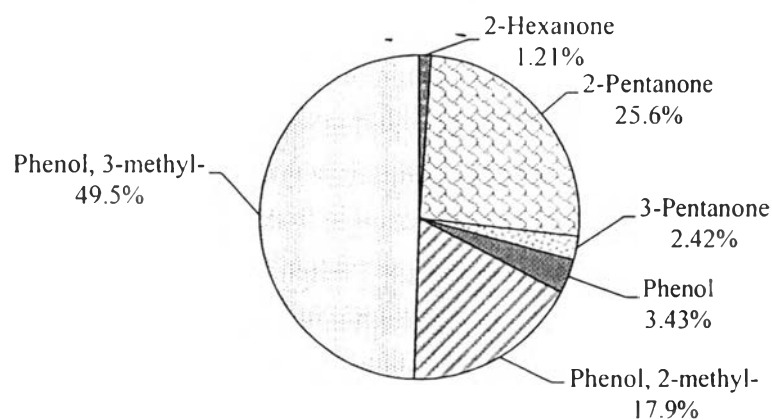

Figure 4.13 Composition of oxygenate compounds (wt%) from using P/HZ5.

Phosphorus oxide is the catalyst for producing oxygenate compounds in the commercial processes such as the production of ethanol from ethylene (Clark, 2002). It is also used in cumene production by using benzene and propylene as raw materials. Moreover, cumene can react further to form acetone and phenol. It can be assumed that phenol and cresol are produced from cumene conversion. However, acetone is not found in this experiment because it can be dissolved in water phase or become a vapor due to its high vapor pressure. There was an evidence that phosphorus oxide could help in the production of phenol and its derivatives. The phosphorus enhanced the phenol production was also revealed by Nowakowski *et al.* (2008). They reported that phosphoric acid and ammonium phosphate can provide the phenol and its derivative in cellulose pyrolysis; however, the uncatalyzed reaction did not yield these phenol compounds.

4.4.4 Effect of Antimony Oxide Promoter

Product distribution and conversion from using Sb/HZ5, Sb/HBeta, and Sb/HY catalysts are shown in Figure 4.14. The oil yield is increased around 4% when antimony oxide is doped to the zeolite. The oil yields can be ranked as followed: Sb/HZ5>Sb/HBeta>Sb/HY. In case of Sb/HZ5(30), new Brönsted acid sites are found together with the decrease of conventional Bronsted acid site after Sb oxides were loaded onto the catalyst as shown in Figure 4.15 A. In addition, the increase of Lewis acid sites is found when antimony oxide is loaded as a promoter. Antimony oxide can act as a Lewis acid site, and partially decreases some Brönsted acid site. So, the oxide can participate in aromatization of light hydrocarbon gases and decrease the cracking reaction, resulting in enhancing the oil yields (Zăvoianu *et al.*, 2003).

Sb/HBeta shows the best performance in kerosene and gas oil production, which are 31.1% and 13.6% in oil, respectively, as shown in Figure 4.16. Sb/HZ5 and pure HZ5 give similar petroleum fractions in the oil products; that are, 94% gasoline, 5% kerosene, and 2% gas oil. Moreover, the production of gas oil and kerosene are enhanced by using Sb/HY as compared to those from HY.
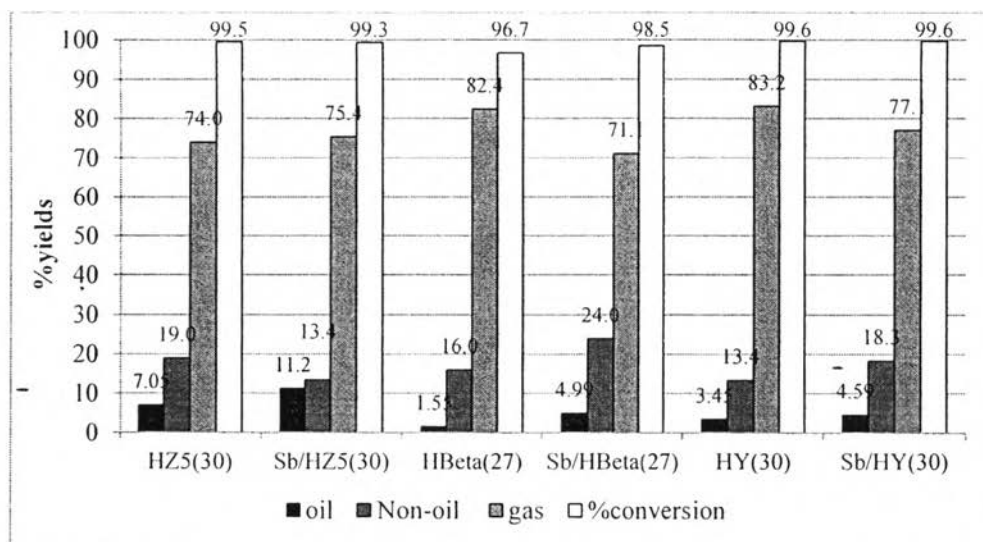
Figure 4.14 Product distribution (wt%) from using Sb/HZ5, Sb/HBeta, and Sb/HY catalysts.
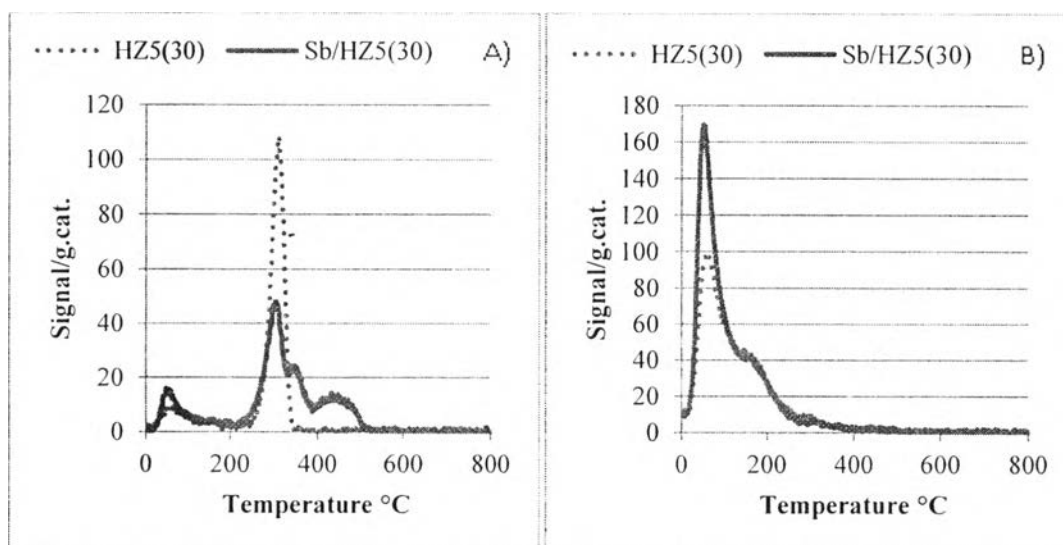
Figure 4.15 Spectra of desorbed propylene (A) and desorbed IPA (B) from using HZ5(30) and Sb/HZ5(30) in TPD-IPA tests.

The xylenes selectivity from using Sb/HBeta is the highest as shown in Figure 4.17. This can be attributed to the suitable pore size and acid properties for the reaction. o-Xylene is decreased significantly from 6.52% to 1.37% in case of using Sb/HZ5. Toluene is increased by using Sb/HZ5; on the other hand, it is

decreased with using large pore size zeolite. The acid properties of antimony oxide improve the catalytic activity of HY and HBeta by enhancing C9 and C10+ aromatic formation. This can occur from disproportionation reaction, which is governed by carbenium ion mechanism.
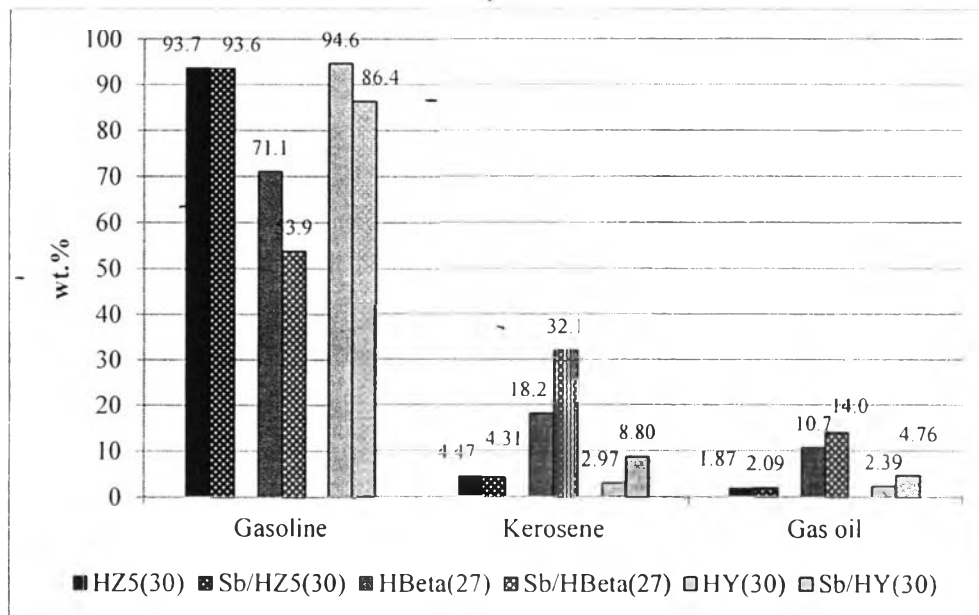

Figure 4.16 Petroleum fractions (wt% in oils) from using Sb/HZ5, Sb/HBeta, and Sb/HY catalysts.

The ratio of p-xylene in xylenes from using Sb/HZ5 is 0.37, which is higher than that of pure HZ5 and other antimony oxide-modified zeolites as shown in Figure 4.18(A). It might be contributed from the penetration of antimony oxide into the pore of HZSM-5 that leads to get the proper pore size for high p-xylene selectivity (Zheng et al., 2003; Xue et al., 2007).

Moreover, the decrease in Bronsted acid site and the external zeolite surface modification are also considered to be responsible for high p-xylene selectivity. Sb/HZ5 gives the best yield in propane, but Sb/HBeta and Sb/HY produce mostly ethylene as shown in Figure 4.18(B). Propane is produced mainly by using Sb/HZ5.
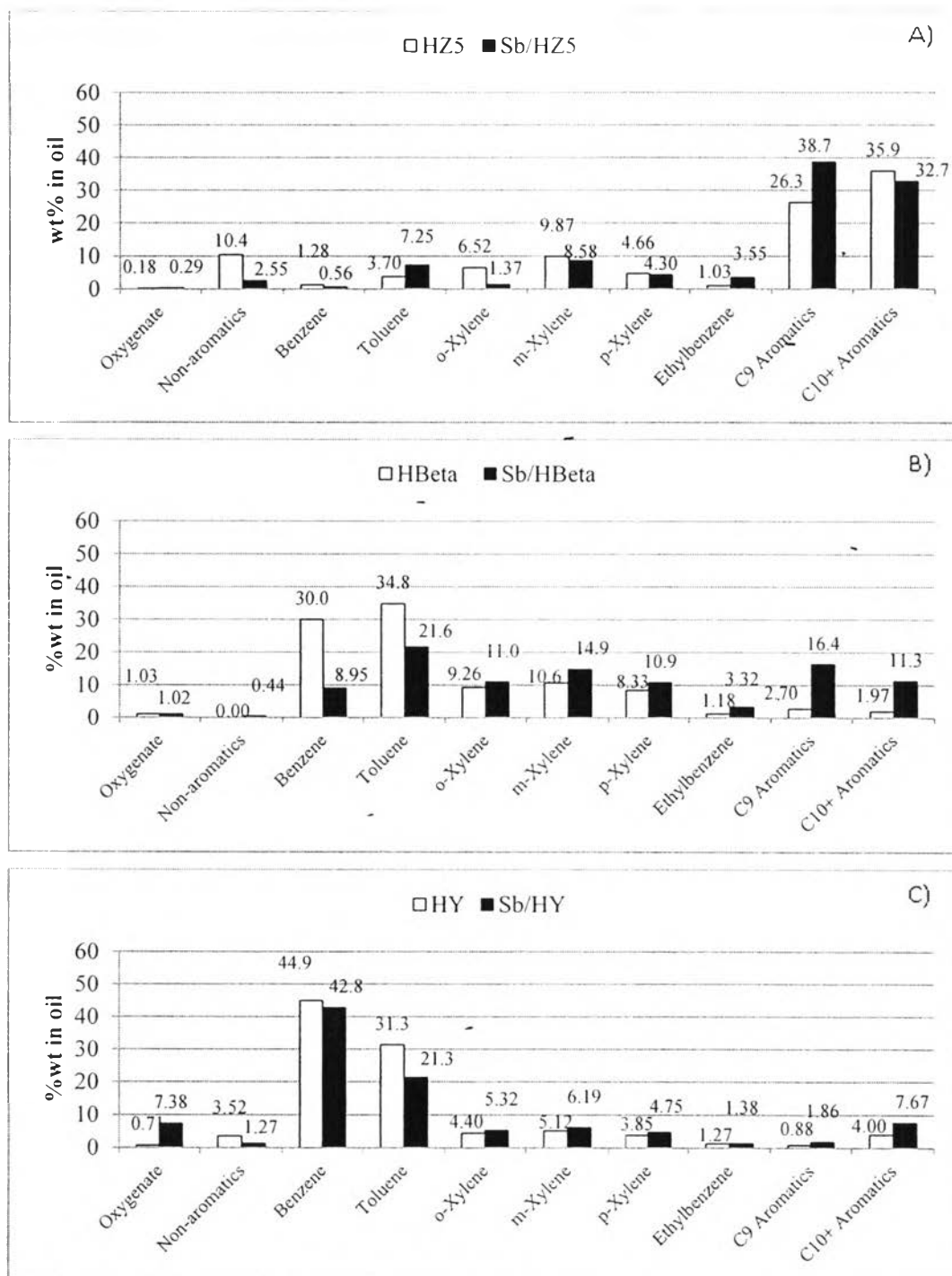
Figure 4.17 Composition of extracted oils from using (A) Sb/HZ5, (B) Sb/HBeta, and (C) Sb/HY catalysts.
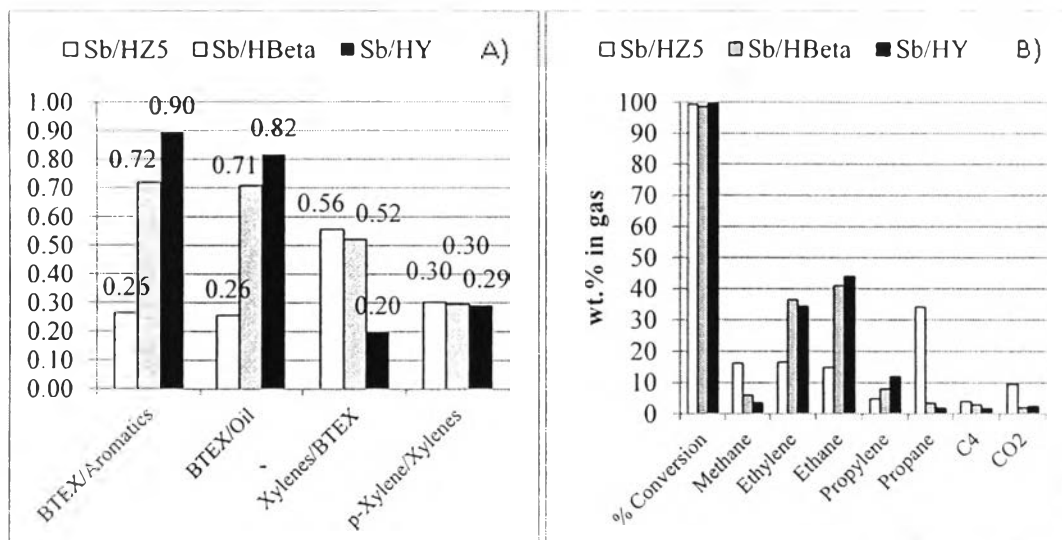
**Figure 4.18** (A) BTEX ratios. and (B) gas product distribution (wt%) of Sb-oxide modified zeolite.

4.4.5 Effect of Bismuth Oxide Promoter

The result shows that bismuth oxide supported on zeolites with moderate and large pore sizes does not affect to the bio-ethanol conversion significantly. More than 99.0% of bio-ethanol is converted to the products. The oil yields are ranked in the order: Bi/HZ5>Bi/HY>Bi/HBeta in Figure 4.19. This ranking follows the same trend as using pure zeolites. The oil yields are increased by 11.9% in case of using Bi/HZ5; but they are increased only 3.18% and 2.42% for Bi/HBeta, and Bi/HY, respectively. On the other hand, Bi/HZ5, Bi/HBeta, and Bi/HY give 2.68, 3.05, and 1.70 times higher oil yield than the corresponding pure zeolites.

The increasing oil yield can be explained by the acid property of modified zeolites. Bi/HZ5(30) has lower Brönsted acid sites density than HZ5(30), however; new stronger Brönsted acid sites are occurred as shown in Figure 4.20. It can be assumed that bismuth oxide can bind to the HZSM-5's Brönsted acid sites, and create three new types of Brönsted acid sites with a higher acid strength. Lewis acid sites seems to change insignificantly when bismuth oxide is loaded to HZ5(30).
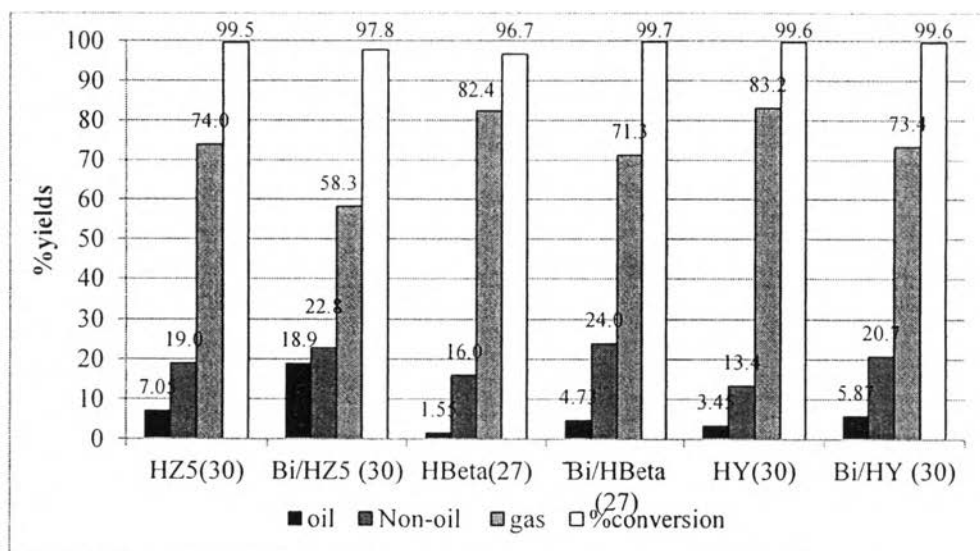
Figure 4.19 Product distribution (wt%) from using Bi/HZ5, Bi/HBeta, and Bi/HY catalysts.
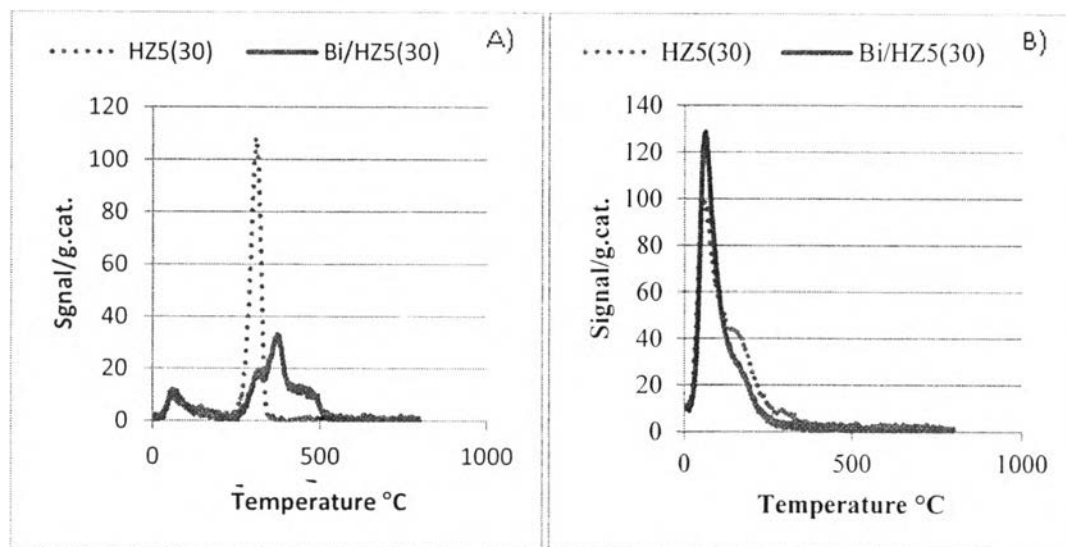
Figure 4.20 Spectra of desorbed propylene (A) and desorbed IPA (B) from using HZ5(30) and Bi/HZ5(30) in TPD-IPA tests.

The distillate product is produced in the order: Bi/HBeta>Bi/HZ5>BiHY as can be seen in Figure 4.21. Although Bi/HBeta can yield kerosene and gas oil mostly, that are 37.2%wt. and 6.4%wt., respectively, Bi/HY and Bi/HZ5 yield the large extent of gasoline. The result shows that HBeta is

the best support when doped by bismuth oxide, which selectively produces kerosene and gas oil. Moreover, *m*-xylene and *p*-xylene are produced in case of Bi/HBeta, which is 21.8%, and 9.3%, respectively as shown in Figure 4.22.
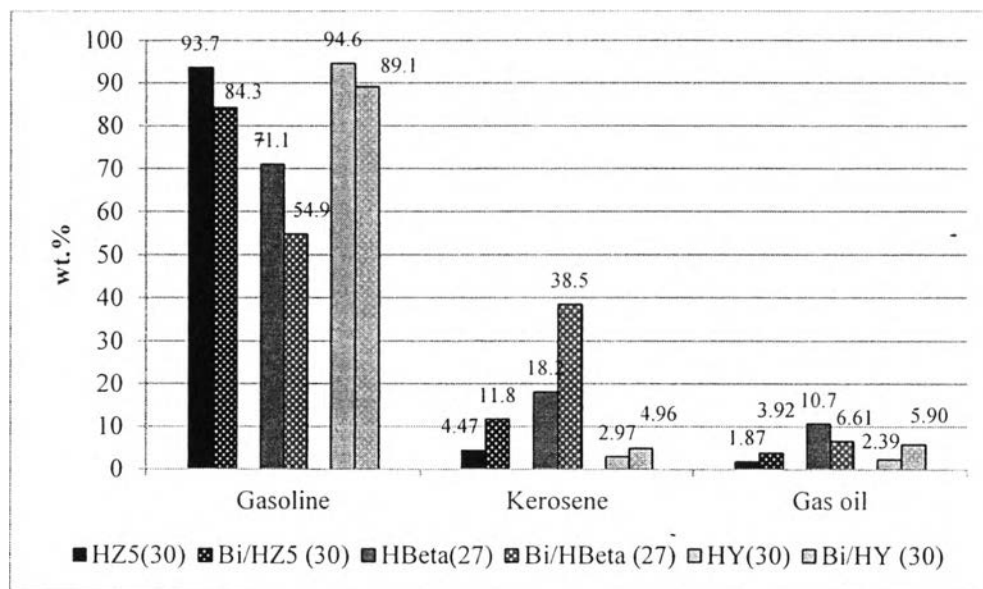

Figure 4.21 Petroleum fractions (wt% in oils) from using Bi/HZ5, Bi/HBeta, and Bi/HY catalysts.

The oil composition falls to the same trend as using antimony oxide promoter. For moderate pore size zeolite, non-aromatics are decreased; on other hand, C8, C9, and C10+ aromatics are increased as shown in Figure 4.22 (A). Benzene and toluene are decreased in case of Bi/HBeta and Bi/HY, but C8, C9, and C10+ aromatics also increased as shown in Figures 4.21 (B) and (C). This makes the ratio of BTEX/oils of Bi/HBeta and Bi/HY decrease. However, in case of using Bi/HZ5, the BTEX/oils ratio is relatively the same because the decrease in non-aromatics.

Propane is obtained by Bi/HZ5 mostly in the gaseous product as shown in Figure 4.23 (B); however, ethylene and ethane are produced mainly by Bi/HBeta and Bi/HY. It can be summarized that bismuth oxide supported on the moderate pore size zeolites tends to produce the large hydrocarbon molecules with

cracking of some of the product to small molecules. The acid property of HZSM-5 still affects to the product even when the zeolite was modified by bismuth oxide.
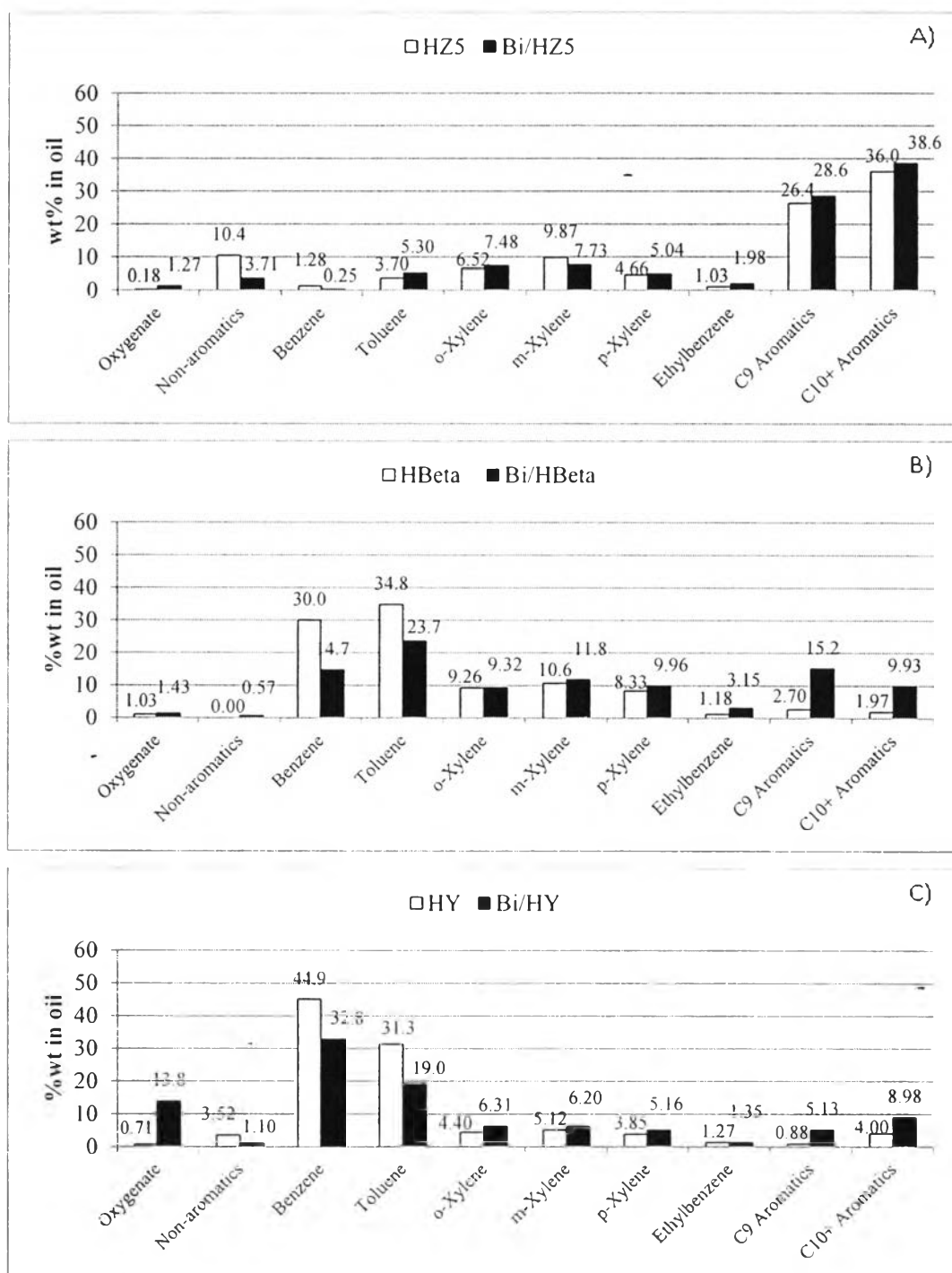
Figure 4.22 Composition of extracted oils from using (A) Bi/HZ5, (B) Bi/HBeta, and (C) Bi/HY catalysts.
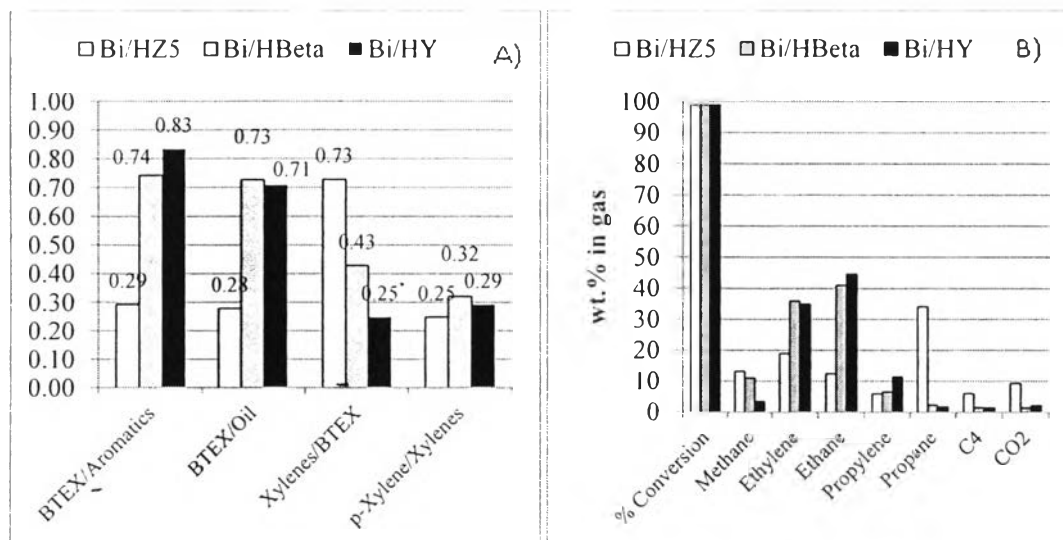
Figure 4.23 (A) BTEX ratios, and (B) gas product distribution (wt%) of Bi-oxide-modified zeolite.

4.5 Conclusions

It can be summarized that the distillate range of product was controlled by the pore size of zeolite, but the quantity also depended on other parameters such as acid strength, and the complexity of the pore. Distillate-range product was produced by large pore size zeolite (46-48% selectivity in all oxide loadings on HBeta). Gasoline was produced by P/HZ5 the most; however, gas oil was produced by P/HBeta the most. Phosphorus oxide-supported zeolites participated in the decrease of oil yield. P/HZ5 produced the highest distillate product collaborated with the production of the large amounts of $C10^+$ aromatic and oxygenate products; however, P/HY and P/HBeta produced the low amount of large hydrocarbon molecules. Moreover, P/HZ5 also showed the yield of phenol and cresol that was around 13.7% in oil. Group 5A oxide promoters can increase the oil yield in all cases, except P/HZ5 since phosphorus oxide decreased the acid density. The oil yield was more improved by bismuth oxide promoter than antimony oxide promoter because Bismuth oxide had higher acid strength than antimony oxide. Bi/HZ5 gave the highest oil yield of 18.9%.

4.6 Acknowledgements

4.7 References

Ali, S.A., Ogunronbi, K.E., and Al-Khattaf, S.S. (2013) Kinetics of dealkylation–transalkylation of C9 alkyl-aromatics over zeolites of different structures. Chemical Engineering Research and Design, 91(12), 2601-2616.

Bi, J., Guo, X., Liu, M., and Wang, X. (2010) High effective dehydration of bio-ethanol into ethylene over nanoscale HZSM-5 zeolite catalysts. Catalysis Today, 149(1–2), 143-147.

Clark, J. "THE MANUFACTURE OF ETHANOL." Chemguide. 2002. 10 August 2013 < http://www.chemguide.co.uk/mechanisms/elim/dhethanol.html>

Cole, J.A., Bittner, J.D., Longwell, J.P., and Howard, J.B. (1984) Formation mechanisms of aromatic compounds in aliphatic flames. Combustion and Flame, 56(1), 51-70.

Costa, E., Uguina, A., Aguado, J., and Hernandez, P.J. (1985) Ethanol to gasoline process: effect of variables, mechanism, and kinetics. Industrial & Engineering Chemistry Process Design and Development, 24(2), 239-244.

de Klerk, A. (2008) Hydroprocessing peculiarities of Fischer–Tropsch syncrude. Catalysis Today, 130(2–4), 439-445.

Furumoto, Y., Harada, Y., Tsunoji, N., Takahashi, A., Fujitani, T., Ide, Y., Sadakane, M., and Sano, T. (2011) Effect of acidity of ZSM-5 zeolite on conversion of ethanol to propylene. Applied Catalysis A: General, 399(1-2), 262-267.

Güell, B.M., Bugge, M., Kempegowda, R.S., George, A. and Paap, S.M. (2012). Benchmark of conversion and production technologies for synthetic biofuels for aviation, SINTEF Energy Research: 93.

Inaba, M., Murata, K., Saito, M. and, Takahara, I. (2006) Ethanol conversion to aromatic hydrocarbons over several zeolite catalysts Reaction Kinetics and Catalysis Letters, 88(1), 135-141.

Johansson, R., Hruby, S., Rass-Hansen, J., and Christensen, C. (2009) The Hydrocarbon Pool in Ethanol-to-Gasoline over HZSM-5 Catalysts. Catalysis Letters, 127(1-2), 1-6.

Madeira, F.F., Gnep, N.S., Magnoux, P., Maury, S., and Cadran, N. (2009) Ethanol transformation over HFAU, HBEA and HMFI zeolites presenting similar Brønsted acidity. Applied Catalysis A: General, 367(1–2), 39-46.

Meng, T., Mao, D., Guo, Q., and Lu, G. (2012) The effect of crystal sizes of HZSM-5 zeolites in ethanol conversion to propylene. Catalysis Communications, 21(0), 52-57.

Moulder, J.F., Stickle, W.F., Sobol, P.E., and Bomben, k.B. (1992) Handbook of X-ray photoelectron spectroscopy: Perkin-Elmer corporation.

Nowakowski, D.J., Woodbridge, C.R., and Jones, J.M. (2008) Phosphorus catalysis in the pyrolysis behaviour of biomass. Journal of Analytical and Applied Pyrolysis, 83(2), 197-204.

Park, J.W., and Seo, G. (2009) IR study on methanol-to-olefin reaction over zeolites with different pore structures and acidities. Applied Catalysis A: General 356(2), 180-188.

Pasomsub, S. (2013) Bio-ethanol dehydration to liquid hydrocarbons. M.S. Thesis, The Petroleum and Petrochemical College, Chulalongkorn University, Bangkok, Thailand.

Resasco, D.E. (2000) Dehydrogenation by Heterogeneous Catalysts. School of Chemical Engineering and Materials Science University of Oklahoma.

Ribeiro, F.R., Alvarez, F., Henriques, C., Lemos, F., Lopes, J.M., and Ribeiro, M.F. (1995) Structure-activity relationship in zeolites. Journal of Molecular Catalysis A: Chemical, 96(3), 245-270.

Sheng, Q., Ling, K., Li, Z., and Zhao, L. (2013) Effect of steam treatment on catalytic performance of HZSM-5 catalyst for ethanol dehydration to ethylene. Fuel Processing Technology, 110(0), 73-78.

Van Vu, D., Miyamoto, M., Nishiyama, N., Egashira, Y. and Ueyama, K. (2006) Selective formation of para-xylene over H-ZSM-5 coated with polycrystalline silicalite crystals. Journal of Catalysis, 243(2), 389-394.

Viswanadham, N., Saxena, S.K., Kumar, J., Sreenivasulu, P., and Nandan, D. (2012) Catalytic performance of nano crystalline H-ZSM-5 in ethanol to gasoline (ETG) reaction. Fuel, 95(0), 298-304.

Wongwanichsin, P. (2013). Modified SAPO-34 for dehydration of Bio-ethanol   to Light Olefins in Comparison with KOH-Treated HZSM-5. M.S. Thesis, The Petroleum and Petrochemical College, Chulalongkorn University,   Bangkok, Thailand.

Xue, N., Chen, X., Nie, L., Guo, X., Ding, W., Chen, Y., Gu, M., and Xie, Z. (2007) Understanding the enhancement of catalytic performance for olefin cracking: Hydrothermally stable acids in P/HZSM-5. Journal of Catalysis, 248(1), 20-28.

Zăvoianu, R., Urdă, A., Bârjega, R., and Angelescu, E. (2003) Comparison Between the Aromatisation of C4 Hydrocarbons on Ga- and Sb-Modified ZSM-5 Zeolites Prepared by Different Techniques. Prog. cat.,12(0), 69.82.

Zhang, L., Wu, J., Chen, F., Li, X., Schoenung, J.M., and Shen, Q. (2013) Spark plasma sintering of antimony-doped tin oxide (ATO) nanoceramics with high density and enhanced electrical conductivity. Journal of Asian Ceramic Societies, 1(1), 114-119.

Zheng, S., Jentys, A., and Lercher, J.A. (2003) On the enhanced para-selectivity of HZSM-5 modified by antimony oxide. Journal of Catalysis, 219(2), 310-319.